Segmentation and Visualization of Brain MRA Images for Image-Guided Neurosurgery

Shuqian Luo, Guangwei Du

Capital University of Medical Sciences
Beijing 100054, China

Abstract

This paper describes a four-stage segmentation and visualization method for MRA volume used for image-guided neurosurgery. This method integrates the anisotropic diffusion filter, the statistical threshold, 3D mathematical morphological operations, surface extraction and the Active Shape Model. A new idea for ASM is proposed that deformation is driven by an Euclidean distance field of image edge.

Keywords: MRA, Segmentation, Active Shape Model, Euclidean Distance Field, Image-guided Neurosurgery

1. Introduction

Image-guided surgery has become indispensable over the last years. By using image-guided technology, a surgeon could preserve normal tissues while maximizing the resection of lesions during cortical surgery. One major challenge of Image-guided surgery is to bring the various facets of medical information such as CT, MRI together into one single environment. Apparently, the more information is obtained by the image-guided surgery system, the more precision can be achieved by the surgery intervention procedure. The visualization of intracranial vessel is extremely important for neuro-surgery. More recently, Magnetic resonance angiography (MRA) as a new angiography technique has been used widely for diagnostic and therapeutical purposes. The integration of the MRA information into the image-guided surgery environment has undoubtedly become an interest problem of image-guided surgery. [1]

The techniques most commonly used for MRA can be classified into two major categories: Time-of-flight and phase contrast MR angiography. Both techniques rely on separate physical effects, and will result in images with different information about the vasculature. Time-of-flight MR angiography is more useful for image-guided neuro-surgery because of its validity in brain vessel and reserved background information. In this paper the Time-of-flight MR angiography is used as an MRA acquisition technique.

In order to achieve a more natural presentation of a given medical dataset, a series of segmentation and visualization techniques have been developed which provide three-dimensional views of the organs of interest. Most of these methods deal with CT or MRI data effectively. But these methods do not work well in MRA because MRA images usually have relative low signal-background intensity ratios.

2. Method

A four-stage strategy is used to segment the total brain MRA dataset. First a statistical analysis of histogram is conducted to generate a mask which separates the foreground from the background. Second, mathematical morphological operators are used to strip skull from brain tissue. The Marching Cubes algorithm is then used to generate the shape surface of scalp, brain and intracranial vessel. Finally, a Euclidean distance field based active shape model (ASM) is adopted to refine the obtained mask. For segmentation of brain tissue from MRA images, we use the combination of gray level, spatial topological characteristic and edge information. Using an active shape deformable model guided by an edge-based Euclidean distance field can effectively eliminate the error introduced by intensity inhomogeneities.

2.1 Segmentation of tissue and background

The procedure to segment tissues from the background consists of two steps. First, the MRA data are processed with an anisotropic diffusion filter to reduce noise and preserve edge information. Then a reasonable threshold is estimated by statistical

histogram analysis to separate tissues from the background.

- ***Nonlinear Anisotropic diffusion Filtering***

The MRA data have low signal-to-noise ratios because non-vessel area signals are depressed for enhancement of vasculature information. The boundaries of brain, skull and other tissues can be obscured by noise.

Anisotropic diffusion filter was proposed by Perona and Malik [3].

$$\frac{\partial}{\partial t} I(p,t) = \nabla \bullet (c(p,t) \nabla I(p,t)) \qquad (1)$$

where I(p,t) is the MRA volume data, p refers to the voxel vector (a point in R^3) and t refers to the iteration step. ∇ is the gradient operator, and $\nabla \bullet$ indicates the divergence operator. $c(p,t)$ is the diffusion coefficient function,which is a monotonically decreasing function of the image gradient magnitude. It allows for locally adaptive diffusion strengths: edges are selectively smoothened or enhanced based on the evaluation of the following diffusion function:

$$c(p,t) = e^{-\|\nabla(p,t)\|^2 / 2k^2} \qquad (2)$$

k is referred to as the diffusion constant and the behavior of the filter depends on k.
For all the images in this paper the value of k = 128 and t = 3 is used.

Estimation of threshold

After anisotropic diffusion filtering, an initial coarse segmentation of the foreground and background is achieved using a sample intensity threshold. The threshold is automatically generated by histogram statistical analysis. We use the following equation to obtain a reasonable threshold:

$$k^* = \arg\max_k (\sigma^2(k)) \qquad (3)$$

where $\sigma^2(k)$ is the statistical dispersion function described by the following equation :

$$\sigma^2(k) = \omega_0(\mu_0 - \mu)^2 + \omega_1(\mu_1 - \mu)^2 \qquad (4)$$

k is the intensity threshold, while ω_0, μ_0 and ω_1, μ_1 stand for probability and average of intensity below and above k respectively. μ refers to the total intensity average of images. Thus, a binary image is produced.

2.2 3D Mathematical morphological operations

The brain can now be segmented by finding the largest contiguous foreground cluster in some of the sample cases. However, the brain is almost always connected with the non-brain tissues such as eyeballs and scalp via thin bridges, often caused by optic nerves, or very narrow skull-brain gaps.
Image morphology provides a way to cope with the misclassification problem caused by thin connections. Several binary morphological operators are used in our segmentation step, such as erosion denoted by Θ, dilation denoted by $\oplus$, conditional erosion denotd by Θ_{cond} and conditional dilation denoted by $\oplus_{cond}$. The conditional morphological operation only change the voxel where Ic = 1, Ic is a second binary image as the operation condition. We also use a maximum connected area selection operator denoted by S_{max}. In these morphological operations, we use a 19-connected 3D structuring element denoted by R. The set of the foreground voxels is denoted as X_{init}={x_k: $I(k) = 1$}, where $I(k)$ is the binary image generated by the above procedure. The objective of the morphological algorithm is to select the voxels corresponding to the scalp, the brain and the intracranial vessels.
The morphological operations of the algorithm are listed in Table 1.

Table 1. Some morphological operations

Operation	Description
$X_D = X_{init} \oplus R$	Dilate the original binary image
$X_{scalp} = X_D \Theta_{cond} R$ ($Ic = X_{init}$)	Conditional Erosion to get the scalp mask using X_{init} as the condition
$X_E = X_{init} \Theta R$	Erode the original binary image
$X_M = S_{max}(X_E)$	Select the largest connected area
$X_{brain} = X_M \oplus_{cond} R$ ($Ic = X_{init}$)	Conditional Dilation to get the brain mask

This stage the mathematical morphological operation in 3D is used to incorporate spatial topology information into segmented image obtained by threshold segmentation. After morphological operation, a sample condition threshold is used to obtain the images of the intracranial vessels.

2.3 Refinement using edge distance field driven ASM

Inhomogeneities of the magnetic fields during image acquisition caused intensity non-uniformities in MRA images. This affected the segmentation precision if the images are obtained based solely on image intensity. Therefore, the segmentation results should be refined by a method that is insensitive to intensity non-uniformities. The well known Marr-Hildreth edge detector is insensitive to local intensity bias. An active shape model algorithm driven by edge Euclidean distance field is then used to refine the generated surface.

- ***Edge detection using Marr-Hildreth***

The Marr-Hildreth edge detector is based on a low pass filter with a symmetric Gaussian kernal, followed by the localization of zero-crossings in the Laplacian of the filtered image. It can be represented as:

$$C(k) = \nabla^2 (I(k) * g_\sigma(p)) \qquad (5)$$

where C is the output contour image, I is an input image, * is the convolution operator, g_σ is a Gaussian kernel with variance σ^2,

$$g_\sigma(p) = e^{-\|p\|^2 / 2\sigma^2} \qquad (6)$$

p is a point in the 3D volume, and ∇^2 is the Laplacian operator. A binary edge image is obtained by using a single threshold in *C(k).* In this work, we use 6 as the threshold and 1.1 as the Gaussian kernel parameter σ.

- ***Calculation of Euclidean distance field***

A physical model for ASM algorithm is provided to refine the segmentation result. Usually an intensity field is used as elastic force to guide the deformation of shape model. In this paper, an Euclidean distance field is obtained from a binary edge image and used as the physical force for ASM algorithm.

Distance fields are expressed as a two or three-dimensional array of values, where each value is the minimum distance to the encoded object [4]. A distance field data set D representing a surface S is defined as D: R^3->R and for p->R^3,

$$D(p) = \mathrm{sgn}(p) \bullet \min(\|p - q\| : q \in S$$
$$\mathrm{sgn}(p) = \begin{cases} -1 & if \quad p \quad inside \\ +1 & if \quad p \quad outside \end{cases} \qquad (7)$$

where ‖ is the Euclidean norm.

In this study, an EVDT algorithm is used to compute the distance field developed by Mullikin [5]. Figure 1 shows the matrix portions used.

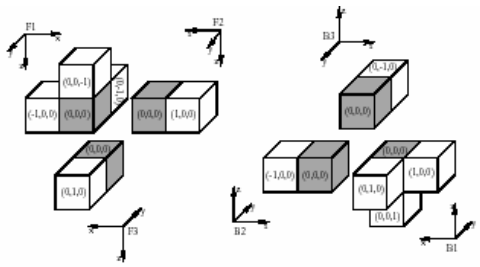

Figure 1. Matrix portions used by the six passes of the EVDT.

- ***Active shape model algorithm***

A deformable shape is a spatial surface that has an initial position and an objective function associated with it. The main idea of this model is that the surface is fitted to the surface of the brain or other structures iteratively. Normally there are two main constraints to the fitting, one that enforces some form of smoothness on the surface (both to keep the surface well-conditioned and to match the physical smoothness of the actual brain surface) and the other that fits the model to the correct part of the image, in this case, the brain surface [2].

In analogy to physical systems, the shape is deformed to minimize its energy over time. This energy of deformable shape is expressed as a sum of two components: its internal energy and its external energy.

$$E_{shape} = E_{\mathrm{int}\,ernal} + E_{external} \qquad (8)$$

The internal energy term imposes a piecewise smoothness constraint on the snake by preserving low first and second derivatives along the surface:

$$E_{\mathrm{int}\,ernal} = \int_S (w_1(s)\|v'(s)\|^2 + w_2(s)\|v''(s)\|^2) ds \qquad (9)$$

where s is surface point vector, v'(s) and v"(s) denote the first and second derivatives along the shape surface respectively. w is a penalty function associated to the surface deformation. w_1 is the coefficient of elasticity, and w_2 is the coefficient of rigidity for the surface. The

external energy function associates the shape to some features of image.

$$E_{external} = -\left\|\nabla I(v(s))\right\|^2 \qquad (10)$$

To find the local minimization of equation (8), the Euler–Lagrange equation should be solved for *v*:

$$-(w_1 v')'+(w_2 v'')''+\nabla E_{external}(v) = 0 \qquad (11)$$

The solution to this differential equation is difficult and time-consuming. In this study, a more practical discrete solution is used:

$$S^t = w_1 s'+w_2 s''+w_3 \nabla I(s) \qquad (12)$$

where S is vector set which represents discrete surface , w is coefficient of deformation, s is an element of S, *I(s)*, in this case is the Euclidean distance field of the edge. In our work, we use w_1=0.6, w_2=0.1, w_3=0.075. The selection of parameter is empirical. The algorithm works well in this condition.

3 Results

OpenGL is used as a 3D engine to visualize results. A fusion of a brain MRI image with the blood vessel system is shown in figure 2.

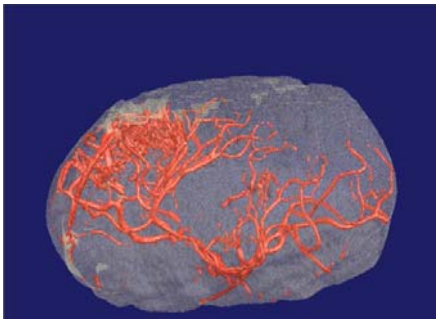

Figure 2. visualization results of our method

Table 2 Time cost of the algorithm

Algorithms	Time(ms)
Anisotropic diffusion filter	42078
Morphological operations	119406
Edge detection	3469
Euclidean distance field generation	5781
Active shape model algorithm	7344

To verify that the method presented in this paper, we use it in our Surgery Planning System, and several MRA volume datasets have been used to test this algorithm. Results showed that this method is effective and robust with intensity inhomogeneities.

All algorithms are implemented in C++ in a dual-CPU workstation with 2GB memory. Table 2 shows the time cost in each step for a 256*256*112 MRA volume dataset.

4 Conclusion

The segmentation and visualization technique presented here shows an effective solution of MRA volume data segmentation. This method can be used in image-guided neurosurgery to improve the accuracy and safety of image-guided neurosurgery intervention. There are a number of unsolved issues that need to be addressed in the brain automatic segmentation. The future works will improve the algorithm speed for real-time image-guided neurosurgery application. More structures segmented automatically are also important to image-guided surgery.

5. Acknowledgment

This work was supported in part by the National Natural Science Foundation of China grant 30270401, and National High Technology Research and Development of China grant 2002AA23121.

6. References

[1] A. Pommert, M. Bomans, K. H. Hohne. Volume visualization of magnetic resonance angiography. IEEE Comput. Graphics Appl. 12 (5), 12-13, September 1992.

[2] Tina Kapur, W. Eric L. Grimson, William M. Wells III, and Ron Kikinis. Segmentation of brain tissue from magnetic resonance images. Medical Image Analysis (1996) volume 1, number 2, pp 109¨C127

[3] Perona, P., and Malik, J. 1990. Scale-space and edge detection using anisotropic diffusion. IEEE Trans. Pattern Anal. Mach. Intell. 12**:**629–639.

[4] B.A. Payne and A.W. Toga. Distance field manipulation of surface models. IEEE Computer Graphics and Applications, 12(1):65–71, January 1992.

[5] J. C. Mullikin. The vector distance transform in two and three dimensions. CVGIP: Graphical Models and Image Processing, 54(6):526–535, 1992.